Source misalignment in multimode polymer tapered waveguides for optical backplanes

Atef M. Rashed, MEMBER SPIE
David R. Selviah
University College London
Department of Electronic and Electrical Engineering
Torrington Place, London WC1E 7JE
United Kingdom
E-mail: a.rashed@ee.ucl.ac.uk

Abstract. Polymer tapered multimode waveguides were modeled using the finite difference wide-angle beam propagation method to investigate whether tapered input waveguide couplers decreasing in width away from the waveguide entrance give improved tolerance to lateral misalignments of an optical source compared to straight waveguides and whether there is any effect on angular misalignment tolerance for use in optical backplane interconnections. Input tapered couplers having a larger entrance and tapering down in width do indeed improve the lateral misalignment tolerance compared to straight waveguides but do so at the expense of an increased loss. Tapers have no effect on angular tolerance for strongly driven vertical cavity surface-emitting laser (VCSEL) sources although they cause a loss of angular tolerance for single-mode fiber sources and VCSELs at low drive currents. *© 2007 Society of Photo-Optical Instrumentation Engineers.* [DOI: 10.1117/1.2432875]

Subject terms: lateral misalignment; angular misalignment; polymer tapered waveguide; optical backplane; FD-BPM; modeling; multimode waveguides.

Paper 050550R received Jul. 12, 2005; revised manuscript received May 16, 2006; accepted for publication Jun. 14, 2006; published online Jan. 26, 2007.

1 Introduction

Large electronic systems are often housed in racks into which are plugged numerous printed circuit board (PCB) cards, variously known as daughter cards, drive cards, blade servers, mezzanine cards, or line cards depending on the application. The daughter cards are plugged into a much larger PCB known as the motherboard or backplane, which supplies power to the daughter cards and more importantly interconnects them at high data rates using multilayer copper tracks. However, at data rates of 10 Gbits/s copper tracks suffer cross talk due to electromagnetic interference (EMI) and can only be used over short distances. This requires complex signal shaping to overcome attenuation and distortion due to high frequency parasitics and limited bandwidths.[1] Polymer waveguides fabricated on or laminated in a hybrid PCB with low data rate copper tracks offer a low cost and compact approach to overcome the limitations of high bit rate copper track interconnections. The optical waveguide interconnections running on or in the backplane connect laser sources on one daughter card to photodiode (PD) detectors on another daughter card.[2] This approach ensures a completely passive backplane as it is easier to remove and replace the daughter cards if an active device on them fails. To avoid the need for costly, precisely aligning optical connectors, the laser sources must couple efficiently and reproducibly to the waveguides even when slightly misaligned[3,4] due to plugging or unplugging the daughter cards or thermal expansion or vibration.

In this paper, we investigate whether the addition of tapered waveguide couplers in which the waveguide width is reduced away from the entrance gives more tolerance to small lateral translations or small angular rotations of the laser source than a uniform width waveguide. We consider a 10 Gbits/s 850-nm vertical cavity surface-emitting laser (VCSEL) source directly butt-coupled to the waveguide tapered coupler. The tapered waveguide coupler is followed by a multimode waveguide of uniform width which is usually considered for use on optical backplanes as it has larger lateral and transverse misalignment tolerances than a single-mode waveguide. We modeled the effect of lateral and angular, in-plane, offsets of an optical source field with respect to the waveguide entrance, on the optical power coupled through. We chose two source fields for comparison of different source divergence from the same area to elucidate the behavior: the output of a multimode VCSEL and the output of a single-mode fiber. The finite difference beam propagation method (FD-BPM) was used to model the propagation of the field along the polymer tapered multimode waveguides,[5] input couplers. Multimode waveguides with large core diameters are often chosen for their potential to provide larger misalignment tolerances. The polymer material is chosen to be suitable for realization of low cost, low loss waveguides over the large area of the backplane.

2 Waveguide Structure and Optical Source

We chose typical parameter values for the waveguides corresponding to the use of Truemode polymer[6] for the core and the cladding. This polymer can be made with a range of refractive indices so we chose the largest refractive index difference between the core and the cladding to give the highest confinement as is commonly chosen for use on optical backplane interconnections. The polymer waveguide layer often has to be laminated between or within a flame retardant 4 printed circuit board, and therefore, the waveguides are formed as buried core structures within a surrounding cladding. The polymer multimode waveguides

modeled had a step index buried channel structure, a core refractive index, $n=1.54$ with a 2% step index difference between core and cladding typical of some optical polymers and a core thickness of 50 μm. The propagation loss was taken to be 0.03 dB/cm, which is typical of such waveguides, at the operating wavelength $\lambda=850$ nm. This value combines the loss due to scattering from any wall roughness present with material dispersion. Waveguide wall roughness was not included in the modeled results, apart from via the propagation loss, so that the effect of the taper alone could be identified. The inclusion of wall roughness would have also necessitated a very fine mesh grid in BPM to take account of the highest spatial frequency component resulting in very long computation times. In geometrical ray optics, the angle between a ray and the normal to the wall of the taper decreases progressively on subsequent reflections until it falls below the critical angle, 78.5 deg, after which it experiences loss. For a Gaussian source placed at the center of the taper (0, 0, 0) propagating along the waveguide with $\theta=0$ deg, the most angled rays at an angle of 7.4 deg, to the waveguide axis only experience one total internal reflection (TIR) before reaching the critical angle and experiencing partial loss from the waveguide for taper angles of $\varphi \geqslant 1.5$ deg. For taper angles of $\varphi=1$ deg, the extreme rays experience two lossless TIRs and for taper angles of $\varphi=0.5$ deg the extreme rays experience four lossless TIRs before the onset of loss.

The waveguides may have lengths as long as 50 cm across the optical backplane. Because the computational overhead can be prohibitive for simulating such lengths, we chose a shorter but representative length of 2 mm for our simulations. This much shorter length affects the magnitude of the output optical power due to propagation loss but should not significantly affect our conclusions for the misalignment tolerance of the input coupler.

Several tapered input coupler waveguide designs were modeled to assess the tolerance to the misalignment of the input optical source. Figure 1(a) shows the first waveguide design modeled, design 1. It consists of a multimode input section that tapers down linearly or quadratically over 1 mm from a width of W_{t1} to 25 μm with a taper half-angle φ. This waveguide coupler is followed by a straight multimode waveguide section of 25-μm width and 1-mm length to have the same overall length as the other coupler design. Several widths of entrance aperture W_{t1} were simulated while maintaining the values of other parameters. This created several tapers with a taper half-angle φ ranging from 0 to 3.5 deg. Figure 1(b) shows the second waveguide design modeled, design 2. This is an input multimode tapered waveguide coupler that tapers down linearly or quadratically over 2 mm from an entrance width of W_{t2} to 25 μm with a taper half-angle φ. Several taper aperture widths W_{t2} were simulated to provide the same values of taper half-angle φ as those simulated for design 1 in order to provide a direct comparison.

Two optical fields were used as sources in the modeling. The first was a weighted four-transverse mode field output from an 8-μm diameter aperture VCSEL, and the second was the fundamental mode of single-mode fiber of 8-μm core. For the VCSEL, the second and the third order modes were taken to be about twice the strength of the first and fourth order modes to approximate similar experimental results. The VCSEL had a larger numerical aperture (NA), or divergence, than the single-mode fiber which allowed us to investigate the effect of different divergences, NAs, of the source while maintaining the same source diameter. The single-mode fiber can also represent a VCSEL in its fundamental lowest order mode. The value of this is that the transverse modes in a VCSEL depend on its temperature and input drive current. At low drive currents, the VCSEL operates in its lowest order mode, and as the drive current increases and the VCSEL heats up, it tends to hop to a higher mode. Therefore, the use of two models for the optical source allows us to deal with low and high current operations of a VCSEL. The input optical fields used in the simulation are shown schematically in Figs. 1(c) and 1(d).

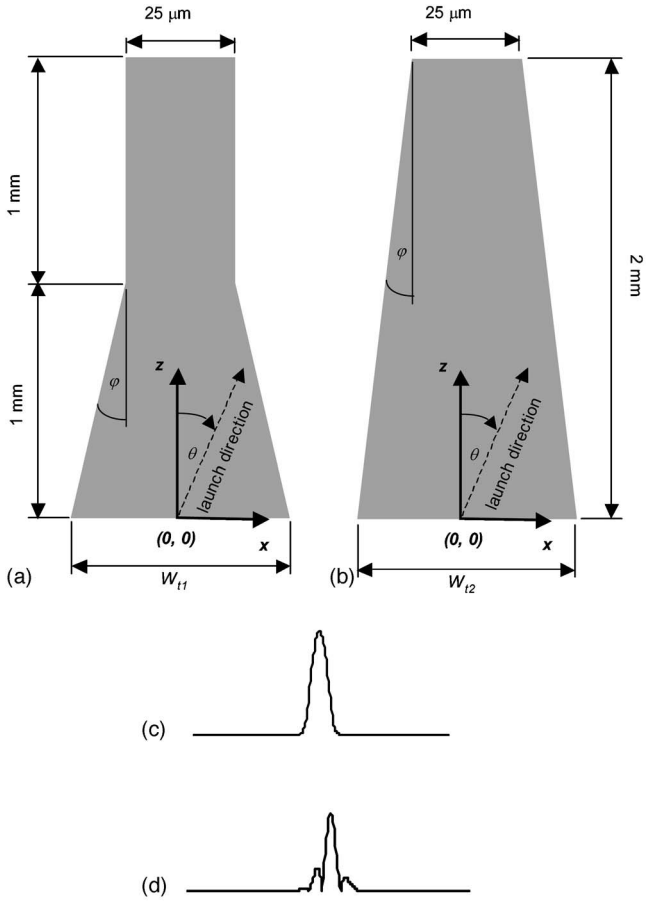

Fig. 1 (a) Design 1, linear taper over 1 mm followed by 1-mm straight section; (b) design 2, linear taper over 2 mm; (c) schematic of the input optical field from a multimode VCSEL; (d) schematic of the input optical field from a single-mode fiber.

The input field is launched into the waveguide structures along the launch direction at angle θ to the z optical axis, shown in Figs. 1(a) and 1(b). Perfect lateral and angular alignment corresponds to the input field launched from the center of the input aperture (0, 0) in the xz plane at angle $\theta=0$ deg. In the simulation, we also assumed a perfect axial alignment along the z axis.[4]

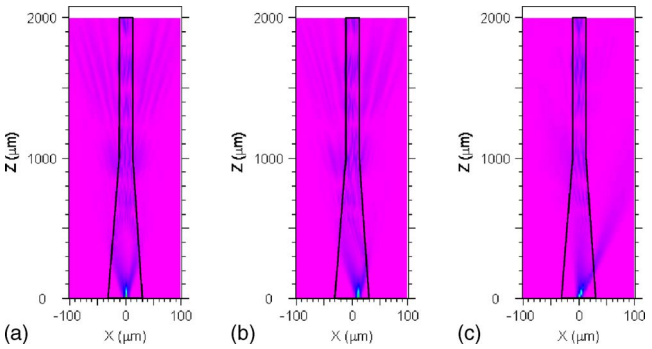

Fig. 2 Propagation of VCSEL input field in linear taper: (a) $W_{t1}=60$ μm, $\varphi=1$ deg, $\theta=0$ deg at (0, 0, 0); (b) $W_{t1}=60$ μm, $\varphi=1$ deg, $\theta=0$ deg at (10, 0, 0); (c) $W_{t1}=60$ μm, $\varphi=1$ deg, $\theta=4$ deg at (0, 0, 0).

3 Numerical Model

The mathematical model used in the simulations is based on three-dimensional FD-BPM (3D FD-BPM). This method employs the following wave equation for the field u:[7]

$$\frac{\partial u_x}{\partial z}=\frac{i}{2\bar{k}}\left\{\frac{\partial}{\partial x}\left[\frac{1}{n^2}\frac{\partial}{\partial x}(n^2u_x)\right]+\frac{\partial^2}{\partial y^2}u_x+(k^2-\bar{k}^2)u_x\right\}, \quad (1a)$$

$$\frac{\partial u_y}{\partial z}=\frac{i}{2\bar{k}}\left\{\frac{\partial}{\partial y}\left[\frac{1}{n^2}\frac{\partial}{\partial y}(n^2u_y)\right]+\frac{\partial^2}{\partial x^2}u_y+(k^2-\bar{k}^2)u_y\right\}, \quad (1b)$$

where x, y, and z coordinates correspond to the lateral, transverse, and propagation directions, respectively. $\bar{k}$ is the reference wave number and $k=(2\pi/\lambda)\ n(x,y,z)$ is the spatially dependent wave number.

Because the waveguide structures are multimode and a range of angular misalignments are considered, rays propagate over a wide range of angles to the optical axis θ. Therefore, the wide-angle form of FD-BPM incorporating the Padé approximation is employed to overcome the paraxial nature of the wave equation.[8,9] We used the Padé (1, 1) approximant[8] to minimize the numerical errors. In the calculations, transparent boundary conditions (TBCs) were implemented[10] to eliminate spurious reflections at the edges of the computation domain.[11]

A numerical mesh with step sizes of $\Delta x=\Delta y=0.3$ μm and $\Delta z=5$ μm is created within the waveguide structure and the wave equation is then integrated forward in z by replacing the partial derivatives with their finite difference approximations.[12] The optical field is successively calculated at each longitudinal step Δz until reaching the end of the waveguide structure. The total power within the waveguide at the output aperture is then determined by computing the integral of the power in the calculated field at the corresponding z position over the waveguide cross section.

4 Results

Figure 2(a) shows an example of the two-dimensional distribution of propagating optical power in the waveguide for design 1 with a linear taper for a VCSEL source with input waveguide aperture width, $W_{t1}=60$ μm, corresponding to a taper half-angle $\varphi=1$ deg and with zero lateral and angular source offsets. Figure 2(a) shows the VCSEL to be emitting the greatest power in two equally angled beams at ±4.2 deg, due to its higher order transverse modes, which reflect several times along the tapered input coupler. When the two beams again intersect, an interference pattern is set up across the waveguide. Bands of fringes are set up at intervals along the taper and at approximately regular intervals in the following waveguide. In the top half of Fig. 2(a), radiating beams can be seen, which tend to come from the region where the taper meets the straight waveguide and in the latter part of the tapered coupler. For rays at ±4.2 deg for a taper half-angle of $\varphi=1$ deg simple geometrical ray optics calculations based on the critical angle found from the core to cladding refractive index difference show that the rays undergo four lossless TIRs before losing energy by transmission through the taper waveguide wall. On each reflection, the original rays are turned through an angle of 2φ away from the waveguide axis so eventually if the taper is long enough, the rays will be incident on the taper wall at an angle less than the critical angle and so will be partially transmitted. This would explain why the radiated beams only start in the latter part of the tapered coupler. The rays angled most from the axis, originally corresponding to higher order modes, will fall below the critical angle first and so experience more loss than the less angled, lower order modes that will only experience loss further along the tapered waveguide. Extremely weak radiated beams do seem to enter the cladding at the first reflection in contradiction to the simple geometric optics theory. The strongest radiated beams coming from the region where the taper meets the straight waveguide are thought to be due to the mismatch in the modal field profiles in the taper and in the straight waveguide, and this is main cause of loss in the taper. It is interesting that the radiated beams in the cladding only exist over a small range of angles at similar angles to the waveguide axis as the original beams emanating from the VCSEL.

To investigate the effect of the taper on source lateral misalignment, several simulations were carried out, each with the source at a different lateral offset along the x axis but at zero y position and directed along the optical axis, $\theta=0$ deg. Figure 2(b) shows a corresponding case to Fig. 2(a) but with a source lateral offset of 10 μm. Figure 2(b) shows similar features to Fig. 2(a) when there was no lateral misalignment: the two beams from the VCSEL; the interference patterns in the latter part of the taper, which occur at intervals along the subsequent straight waveguide at almost the same propagation distances as in Fig. 2(a); the radiated beams from the latter part of the taper and the strongest beams radiating from the joint with the straight waveguide; extremely weak beams radiating into the cladding at the first reflection within the taper. However, in this case, the energy distribution is asymmetric with apparently more radiated beams in the cladding on the side to which the source is offset suggesting that there may be a slightly higher loss.

The source angular misalignment was simulated by positioning the source at the center of the waveguide input aperture (0, 0, 0) but directed along different launch directions with different angles, θ to the z axis. Figure 2(c) shows a corresponding case to Fig. 2(a) but with source

angular offset of 4 deg. In this case, as with the previous one, the laser emits two angled beams, but one of the beams is directed almost along the optical axis and so passes straight along the waveguide taper and into the straight waveguide. Very little radiated light is seen from the latter part of the taper and from the joint between the taper and the straight waveguide, and what little can be seen radiates from the opposite waveguide side to that toward which the VCSEL is directed. The other beam is almost totally transmitted through the wall of the taper because it is incident at less than the critical angle and lost. The patterns of interference can again be seen in the latter part of the taper and in the following straight waveguide at similar positions along the axis as in the aligned case, which is somewhat surprising as the beam is quite differently angled. Although half of the VCSEL's light is lost at the first reflection, this may be counterbalanced by the reduction in loss due to mode mismatch later, and to evaluate this, the power remaining in the waveguide must be calculated by integration across the aperture as in Figs. 4 and 6 for taper coupler designs 1 and 2, respectively.

The output power normalized to the input power is plotted versus the source lateral misalignment in Fig. 3(a) for design 1 with a linear taper, single-mode fiber source and $W_{t1}=60$ μm corresponding to $\varphi=1$ deg. The maximum power is 0.89 corresponding to a lowest loss of 0.5 dB. The loss is fairly flat with misalignment increasing slightly for lateral misalignments more than ±5 μm but remaining low until ±25 μm when it increases rapidly. Therefore, there is a large tolerance to lateral misalignments. Here, we define the lateral offset tolerance for any waveguide structure as the full width at half maximum (FWHM) of the normalized output power as shown in Fig. 3(a) corresponding to the 3-dB width. In this figure, it approximately matches the taper entrance width $W_{t1}=60$ μm. The weak light recorded beyond ±35 μm at a loss of more than −15 dB is surprising as the single-mode fiber source is beyond the width of the entrance aperture. Therefore, this must represent light coupling back into the waveguide through its walls and is indicative of the level of cross talk that may be expected from adjacent guides. Lateral misalignment simulations were repeated for each of the two optical sources and for each of the two tapered coupler designs with different input aperture widths, W_{t1} and W_{t2}, over the range of taper half-angles of $0 \text{ deg} \leqslant \varphi \leqslant 3.5$ deg.

Similar simulations were performed launching the source at different angles θ while keeping the source positioned at the center of the waveguide entrance (0, 0, 0). The output power normalized to the input power is plotted versus the source angular misalignment in Fig. 3(b) for design 1 with linear taper, fiber source, and $W_{t1}=60$ μm corresponds to $\varphi=1$ deg. In this case, the form of the curve is quite different to that for lateral misalignment as any angular rotation causes a rapid increase in loss. So the waveguide tapers are much more sensitive to angular rotations than lateral misalignments. Almost no signal is detected for angular rotations of more than ±7 deg. We define the angular misalignment tolerance for any waveguide structure as the FWHM of the normalized output power as shown in Fig. 3(b). Angular misalignment simulations were repeated for each of the two optical sources and for each of the two

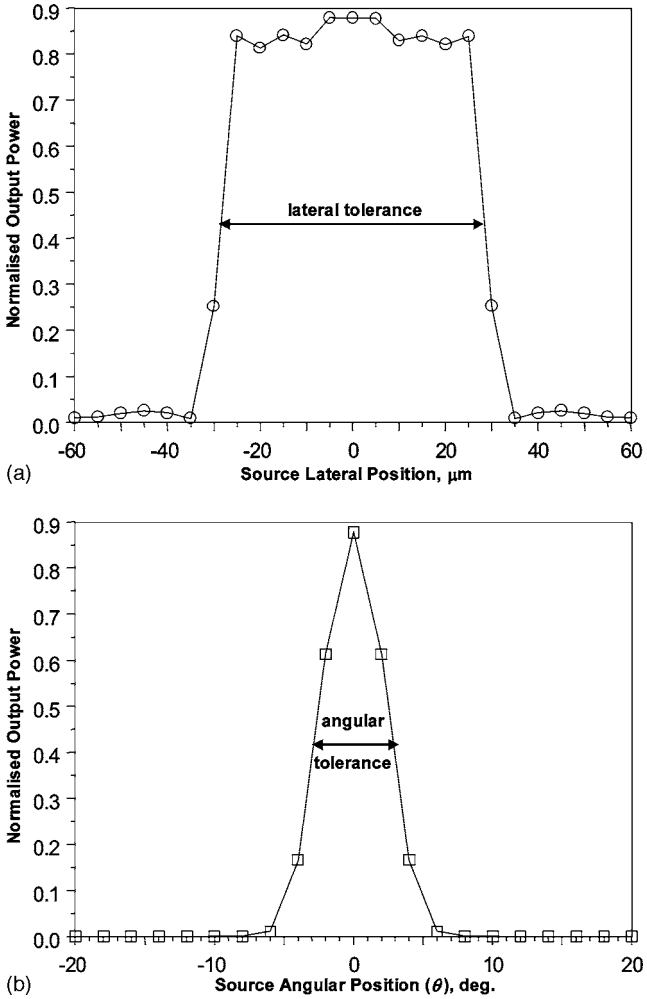

Fig. 3 (a) Output power versus source lateral position, linear taper $W_{t1}=60$ μm, $\varphi=1$ deg, fiber source, $\theta=0$ deg; (b) output power versus source angular position, linear taper $W_{t1}=60$ μm, $\varphi=1$ deg, fiber source at (0, 0, 0).

designs with different waveguide entrance aperture widths, W_{t1} and W_{t2}, over the range of taper half-angles, $0 \text{ deg} \leqslant \varphi \leqslant 3.5$ deg.

To compare the performance for the two different source types with different divergences at various positions and orientations for each taper coupler design and for each taper type, the simulation results are combined together. For design 1, Figs. 4(a)–4(c), show the waveguide lateral tolerance, output power, and angular tolerance, respectively, as a function of taper half-angle φ and input aperture width W_{t1} for linear and quadratic tapers with the more divergent VCSEL source. Figure 5 is the corresponding figure with the less divergent single-mode fiber source. Figures 6 and 7 are the corresponding figures for taper coupler design 2. The output powers are calculated for a source on axis with the output directed along the waveguide axis.

5 Discussion

In 10-Gbits/s optical backplane applications, the diameters of the VCSEL and PD apertures can be about 9 and 75 μm, respectively. The waveguide tapered coupler design requires that at the VCSEL end, the waveguide width (WG)

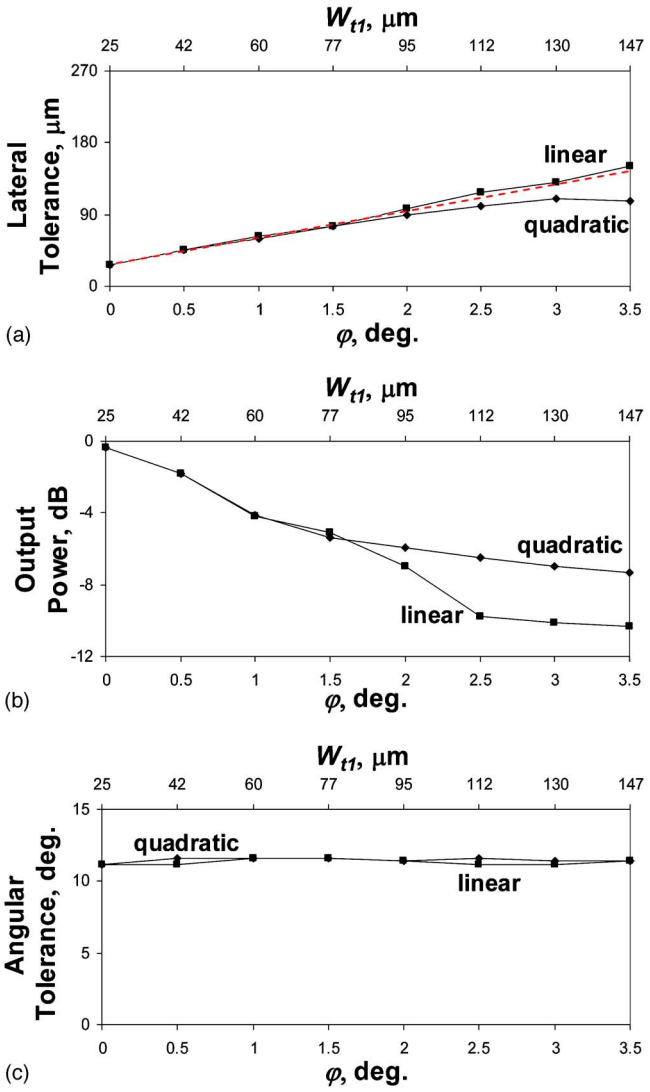

Fig. 4 (a) Lateral tolerance versus φ and W_{t1}, design 1 with VCSEL source; (b) output power versus φ and W_{t1}, design 1 with VCSEL source; (c) angular tolerance versus φ and W_{t1}, design 1 with VCSEL source.

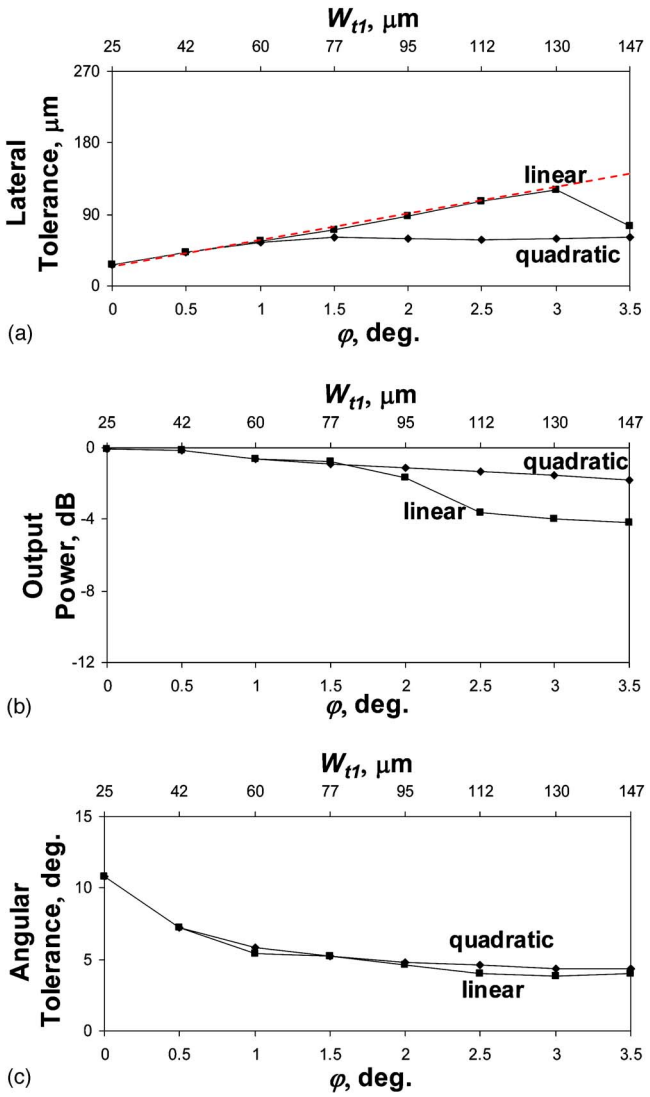

Fig. 5 (a) Lateral tolerance versus φ and W_{t1}, design 1 with fiber source; (b) output power versus φ and W_{t1}, design 1 with fiber source; (c) angular tolerance versus φ and W_{t1}, design 1 with fiber source.

should be large enough to allow easy lateral alignment. At the PD end, the WG should also be smaller than the PD to avoid losses. Due to the large size difference between the VCSEL and the PD, we have chosen to compare 25-μm-wide straight multimode waveguides (for which the apertures are in the ratio VCSEL$<$WG$<$PD over the entire length) with two designs of linearly and quadratically tapered waveguides (for which the apertures are in the ratio VCSEL$<$WG at one end and WG$<$PD at the other).

In terms of lateral tolerance for the VCSEL source, tapered structures always perform better than the straight waveguide (φ=0 deg) as indicated by the positive slope of the curves in Figs. 4(a) and 6(a). The greater lateral tolerance of design 2, Fig. 6(a), compared to design 1, Fig. 4(a) by a factor of 2, is simply due to the larger input aperture width of design 2. Figures 4(a) and 6(a) both show a linearly increasing lateral tolerance with a taper half-angle. The linear taper performs better than the quadratic taper in terms of lateral tolerance particularly for larger taper half-angles. The dotted line plotted on Figs. 4(a), 5(a), 6(a), and 7(a) is a line of unity slope for which the lateral tolerance is equal to the entrance width. The conclusion is that within the modeling accuracy, the 3-dB lateral tolerance of a linear taper is the same as the width of the tapered waveguide entrance and is independent of our choice of taper design. The largest entrance aperture gives the largest lateral tolerance.

For a single-mode fiber source, the lateral tolerance increases with the taper angle until 2 deg$<\varphi<$3 deg, depending on the design, where the lateral tolerance starts to decrease as shown in Figs. 5(a) and 7(a). For taper angles less than these values, the curve closely follows the dotted unity slope curve. The quadratic taper shows much less lateral tolerance for taper angles more than 1 deg. Linear tapers show an optimum value for lateral tolerance at taper angles of 3 deg for design 1 and 2 deg for design 2. For

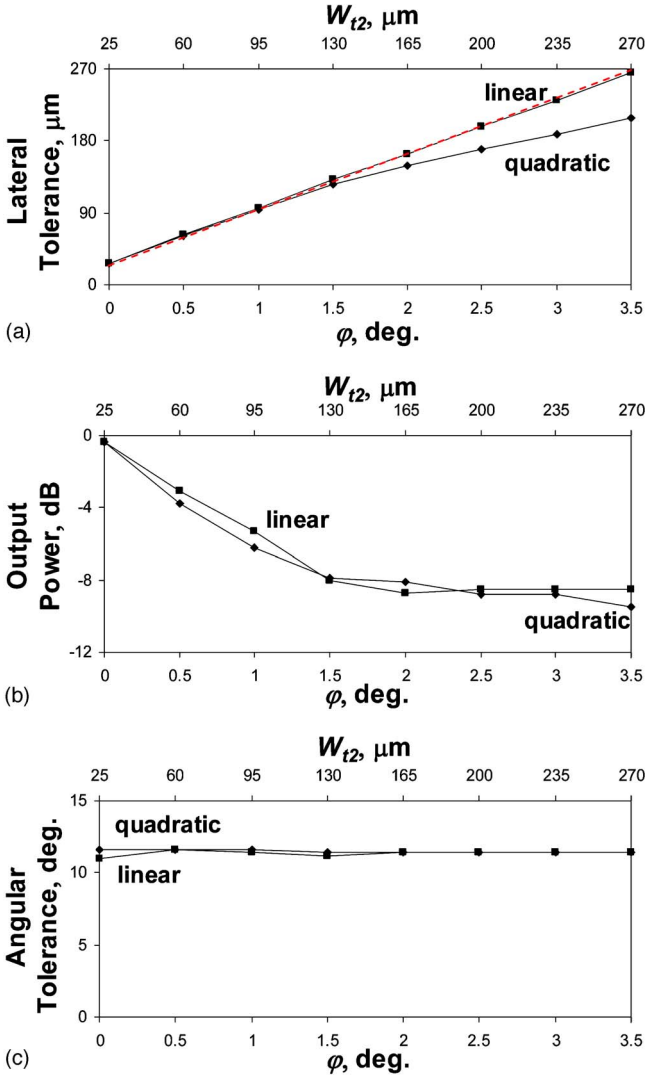

Fig. 6 (a): Lateral tolerance versus φ and W_{t2}, design 2 with VCSEL source; (b) output power versus φ and W_{t2}, design 2 with VCSEL source; (c) angular tolerance versus φ and W_{t2}, design 2 with VCSEL source.

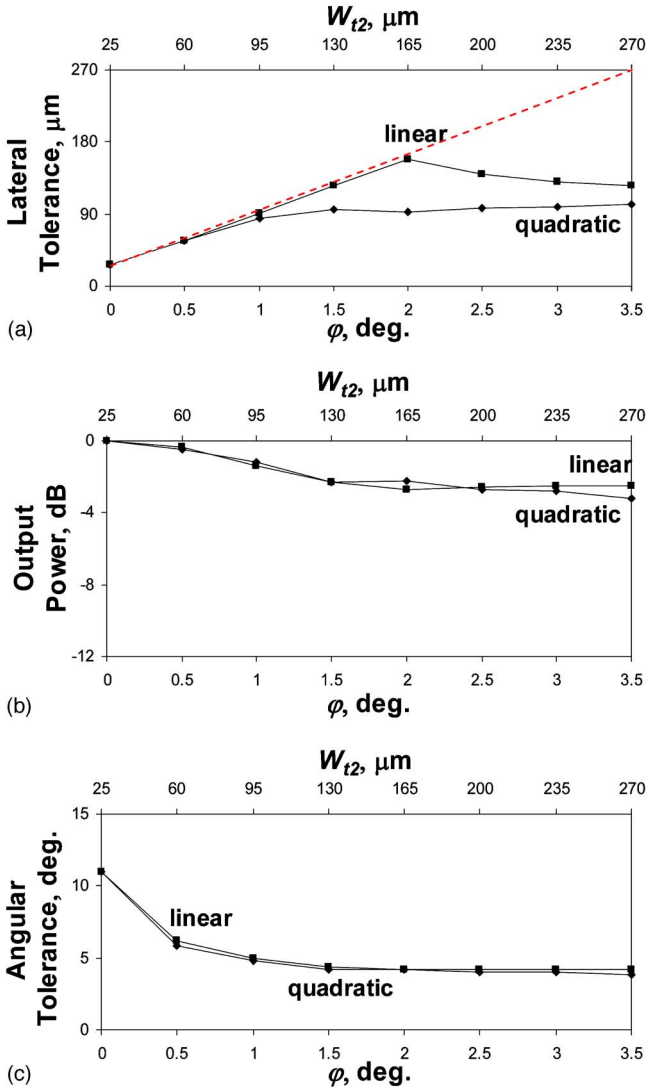

Fig. 7 (a) Lateral tolerance versus φ and W_{t2}, design 2 with fiber source; (b) output power versus φ and W_{t2}, design 2 with fiber source; (c) angular tolerance versus φ and W_{t2}, design 2 with fiber source.

taper angles larger than these optimum values, the lateral tolerance is less than the entrance width of the waveguide, which is somewhat surprising and requires further investigation. For the VCSEL source, Figs. 4(b) and 6(b) show two regions. In the region $\varphi \leqslant 1.5$ deg, the insertion loss increases almost linearly with taper angle. There is a direct trade-off between lateral tolerance and loss for the shallower taper angles, $\varphi \leqslant 1.5$ deg. Figures 4(b) and 6(b) also show that straight waveguides have lower loss than tapered ones, although tapers with shallow angles also have acceptable losses. In the second region for larger taper angles, $\varphi > 1.5$ deg, the rate of increase of loss reduces and it begins to saturate. Although the loss tends to saturate at large taper angles, the lateral tolerance continues to improve. However, the saturation value of loss of ~9 dB is too large to consider operating in this region. For design 1, the quadratic taper has less loss but also less lateral tolerance from Fig. 4(a).

For a single-mode fiber source, Figs. 5(b) and 7(b) show an increase in loss with taper angle similar to that for the VCSEL, but the magnitude of the loss is far less than that for a VCSEL source. Single-mode fibers couple with much less loss than a VCSEL to straight or tapered waveguides. The optical loss surprisingly does not show any sudden changes that correspond to the reduction of lateral tolerance with a taper angle.

Figures 4(c) and 6(c) show that for the VCSEL source, the angular tolerance is almost independent of the taper half-angle at a value of about 11 deg. Figures 5(c) and 7(c) show that for the single-mode fiber source, the angular tolerance decreases with the taper half-angle until $\varphi = 1$ deg, where it reaches a plateau at an angular tolerance of about 6 deg. The single-mode fiber source would be expected to have a narrower divergence, and as it is tilted, more of the beam is transmitted through the waveguide side walls. In the case of the VCSEL source that has a wider divergence and two beams when the VCSEL is tilted, although one

beam exits the waveguide side wall, the other beam couples more efficiently to the straight waveguide with less loss (as we saw in the last Sec. 4), exactly counterbalancing each other.

6 Conclusions

We modeled the propagation of optical fields within several tapered waveguide input coupler structures to study the effect of optical source lateral and angular misalignments. Within the modeling accuracy, the 3-dB lateral tolerance of a linear taper is the same as the width of the tapered waveguide entrance and is independent of our choice of taper design. The largest entrance aperture gives the largest lateral tolerance. For VCSEL sources, straight waveguides have lower loss than tapered ones, although tapers with shallow angles, $\varphi \leqslant 0.5$ deg also have acceptable losses. We conclude that tapers with shallow half-angles of $\varphi \leqslant 0.5$ deg give low loss but that longer tapers are required to give a large entrance width to give a large lateral tolerance and the difference between the lengths of the two taper designs shows that increased taper length results in increased loss. For the VCSEL source, Figs. 4(b) and 6(b) show two regions. In the region $\varphi \leqslant 1.5$ deg the insertion loss increases almost linearly with the taper angle. There is a direct trade-off between lateral tolerance and loss for the shallower taper angles, $\varphi \leqslant 1.5$ deg as they have opposite sign linear slopes. Single-mode fibers couple with much less loss than a VCSEL to straight or tapered waveguides. The VCSEL has better angular tolerance of 11 deg than a single-mode fiber source that reduces to 6 deg at larger taper half angles. In the case of the VCSEL source that has a wider divergence and two beams when the VCSEL is tilted, although one beam exits the waveguide side wall, the other beam couples more efficiently to the straight waveguide with less loss, exactly counterbalancing each other and giving a complete insensitivity to angular misalignments. Quadratic tapers do not appear to offer any advantages over linear tapers. There is no particular advantage of one of the taper designs over the other.

Therefore, we have shown using FD-BPM 3D modeling for typical dimensions and waveguide parameters for buried multimode polymer waveguides that input tapered couplers having a larger entrance and tapering down in width do indeed improve the lateral misalignment tolerance compared to straight waveguides but do so at the expense of an increased loss. Tapers have no effect on angular tolerance for strongly driven VCSEL sources although they cause a loss of angular tolerance for single-mode fiber sources and VCSELs at low drive currents.

Acknowledgments

The authors appreciate the financial support of U.K. Engineering and Physical Sciences Research Council and Department of Trade and Industry via the LINK Storlite project and the fruitful collaboration with Xyratex, Havant, United Kingdom.

References

1. F. Mederer, R. Michalzik, J. Guttmann, H.-P. Huber, B. Lunitz, J. Moisel, and D. Wiedenmann, "10 Gb/s data transmission with TO-packaged multimode GaAs VCSELs over 1 m long polymer waveguides for optical backplane applications," *Opt. Commun.* **206**, 309–312 (2002).
2. J. Moisel, "Optical backplane for avionic applications using polymer multimode waveguides," *Proc. IEEE LEOS Conf.*, **2**, 567–568 (2000).
3. A. M. Rashed and D. R. Selviah, "Modelling of polymer taper waveguides for optical backplane," Proc. of Semiconductor and Integrated Optoelecronics Conf., (SIOE'04), 2004, Cardiff, Wales, Paper 40.
4. W. B. Joyce and B. C. DeLoach, "Alignment of Gaussian beams," *Appl. Opt.* **23**(23), 4187–4196 (1984).
5. A. M. Rashed, K. A. Williams, P. J. Heard, R. V. Penty, and I. H. White, "Tapered waveguide with parabolic lens: Theory and experiment," *Opt. Eng.* **42**(3), 792–797 (2003).
6. Truemode polymer parameters, private communication with Navin Suyal, Exxelis Ltd.
7. W. P. Huang and C. L. Xu, "Simulation of three-dimensional optical waveguides by a full-vector beam propagation method," *IEEE J. Quantum Electron.* **29**(10), 2639–2649 (1993).
8. I. Ilić, R. Scarmozzino, and R. M. Osgood, Jr., "Investigation of the Padé approximant-based wide-angle beam propagation method for accurate modeling of waveguiding circuits," *J. Lightwave Technol.* **14**(12), 2813–2822 (1996).
9. Y.-P. Chiou and H.-C. Chang, "Analysis of optical waveguide discontinuities using the Padé approximants," *IEEE Photonics Technol. Lett.* **9**(7), 964–966 (1997).
10. G. R. Hadley, "Transparent boundary condition for the beam propagation method," *IEEE J. Quantum Electron.* **28**, 363–367 (1992).
11. I. Ilić, R. Scarmozzino, R. M. Osgood, Jr., J. T. Yardley, K. W. Beeson, and Michael J. McFarland, "Modeling multimode-input star couplers in polymers," *J. Lightwave Technol.* **12**(6), 996–1003 (1994).
12. Y. Chung and N. Dagli, "An assessment of finite difference beam propagation method," *IEEE J. Quantum Electron.* **26**(8), 1335–1339 (1990).

Biographies and photographs of the authors are not available